EFFECT OF TEMPERATURE ON FLOW CHARACTERISTICS IN SUPERSONIC IMPINGING JET USING RANS/ILES HIGH RESOLUTION METHOD

L.A. Benderskiy
Central Institute of Aviation Motors, Russia
Leosun.Ben@gmail.com

Keywords: *effect of temperature, supersonic impinging jet, RANS/ILES*

Abstract

This article studies an influence of total temperature at a nozzle inlet on supersonic impinging jet's flow and turbulence parameters by using the RANS/ILES high resolution method. Three temperatures of jet (300K, 400K and 600K) are compared in terms of averaged and fluctuation flow parameters distribution along the jet axis and at the plate. Additionally temperature fluctuations at the wall are indicated. Results of the research are compared with an experimental data and other authors' calculations. Calculation results show that the flow parameters and turbulence on the jet axis have no sufficient dependence with jet temperature. On the other side, there is a nonmonotonous dependence between the total jet temperature at the nozzle inlet and temperature fluctuations on the plate outside the recirculation zone, which can widely vary.

1 Introduction

Impinging jets are found in many engineering applications, e.g. aircraft vertical takeoff and landing, rocket launch, jet cooling. Tone-producing modes are possible; it has depended on the jet exit distance to the plate and nozzle pressure ratio. The supersonic jet produces strong unsteady shock and thermal loads on the plate. The high overall sound pressure level (OASPL) associated with supersonic impinging jets is one of the main sources of noise pollution. That shows the importance of studying the interaction of jets and the flat plate.

Many experiments carried out with cold jet. For engineering applications, it is also important to study the effect of temperature on the flow and characteristic of such jets. Experiments with hot jet are more difficult than studying cold jets. Experimental studies, both cold and hot jets are usually limited in the set of investigated parameters and their location. In the work [1] investigated the influence of a nozzle geometry and the Reynolds number on heat transfer characteristics on the plate. Authors in [2] considered average and fluctuation characteristics of pressure and temperature on the plate and the noise in the far field, depending on the jet temperature. Computer simulation became more common in recent years. In particular, LES method finds the increasing application for the calculation of various flows, as it allows get many characteristics for the analysis of phenomena: averaged parameters, fluctuation of velocity, pressure and temperature, fluctuation spectrum at any point in the computational domain, and allows studying transient phenomena. For example, LES successfully used for the calculation of jet impinging on the plate in [3-6]. The authors of [6] showed complementarity of simulation and experiment. RANS method does not provide complete situation of the phenomenon and wide field for analysis. Also the work of [7] shows that the use of RANS and k-ω turbulence model for calculating of jet impinging on the flat plate leads to errors, because RANS overestimates the heat flux at the stagnation point of the jet.

Thus, LES is interesting for a variety of studies. The main constraint is the computing power. For example, for calculating the jet flow together with the nozzle flow, it is necessary to resolve the boundary layer at the nozzle walls, which can be expensive for high Reynolds numbers. Estimations made in [8] talking about grid contained 10^9 cells. There are examples of calculations on grids of 130×10^6 [3], 400×10^6 [9] and 700×10^6 [4] cells. Calculations on these grids are quite expensive. An alternative approach is to use a hybrid RANS/LES–methods [10, 7], where the flow near the walls is calculated using RANS and turbulence models, and the core flow is calculated by LES method. An additional increase in the method efficiency is achieved with applying high-resolution schemes for the calculation of flow parameters on cell faces [10]. This approach allows the use of much coarser grid for the calculations and provides a good agreement with experiment [10, 11] even at high Reynolds numbers.

The purpose of this work is study the effect of supersonic impinging jet temperature on flow and turbulence characteristics in the jet and near the plate.

2 Numerical method

The method is based on Navier-Stokes equations describing the flow of a compressible gas. The transport equation for turbulence model is written in conservative form for curvilinear coordinate system. The grid lines coincide with the boundaries of computational domain, the nozzle surface and the flat plate. Hybrid RANS/ILES–method is used to solve equations. The RANS method is used near walls and ILES is used in the rest of the computational domain. Scheme viscosity plays a role of a subgrid scale (SGS) model. The Roe method was applied to calculate non-viscous flux on cell faces. The high resolution of this method is provided by using a monotone difference scheme MP9 [12] with upwind 9th-order approximation to calculate flow parameters on cell faces. This approach has been successfully used in [13]. Diffusion fluxes are calculated on cell faces with second-order approximation by central differences. The time discretization is made with second order by implicit scheme and with integration by double-time method. The Spalart–Allmarasa turbulence model [14] is used in RANS region. The WENO–5 scheme [12] is used to calculate convective flows on cell faces in the difference analog of turbulence model equation. In LES region, the Spalart–Allmarasa turbulence model is modified so that the turbulent viscosity is equated to zero. This is achieved by changing the distance dissipative term of turbulence model equation. The modified distance $\tilde{d}$ is calculated by the formula:

$$\tilde{d} = \begin{cases} d, & d \le C_{DES}\Delta_{MAX} \\ 10^{-6}L_{ref}, & d > C_{DES}\Delta_{MAX} \end{cases},$$

where d – the distance from the wall to the cell center, Δ_{MAX} – the maximum size of the cell, C_{DES}=0.65 and L_{ref} – characteristic dimension of the simulation.

This method has worked well in the calculation of sub- and supersonic jets from nozzles of different configurations [10, 11].

3 Simulations parameters

Calculations were carried out in a structured grid containing 1.3×10^6 cells. Computational domain is shown in Fig. 1. The longitudinal cell size near the nozzle exit is 0.03D (D – diameter of nozzle exit). The grid contains 80 cells in the azimuthal direction. Color-coded boundary conditions could be seen in Fig. 1: green – wall function/no-slip wall, red – the entrance to the nozzle, given the total pressure and temperature and the angle of the velocity vector. Orange – outlet boundary condition (parameters extrapolation). The computational grid step to the boundary of the computational domain increases to exclude reflections from the outlet boundary. Blue – the far field asymptotic of the jet [15]. The nozzle geometry close to the geometry described in [16].

Flow mode corresponds to NPR = 4.03 (nozzle pressure rate). Dimensionless distance from the nozzle to the plate is h/D = 4.16. Jet calculations made for cases with the total temperature (T_{in}) at the nozzle inlet equal to 300K, 400K and 600K. Pressure and temperature in the surrounding area are P_{amb} = 1 bar and T_{amb} = 300K. The plate was considered as an adiabatic wall. Dimensionless time step, adiabatic velocity at nozzle exit and other simulation parameters are show in Table 1.

Table 1. Simulation parameters.

T_{in}, K	NPR	M_j	U_j, m/s	$\frac{\rho_j U_j^2}{2}$, Pa	Re× 10^{-6}	$\frac{\Delta t U_j}{D}$
300	4.03	1.56	445	171209	1	0.011
400			514		0.86	0.013
600			629		0.64	0.016

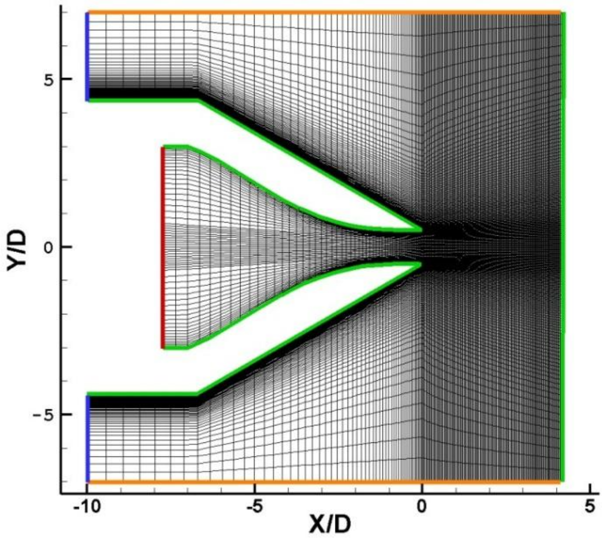

Fig. 1. Longitudinal section of computational grid.

3 Simulation results

The jet flow is calculated enough detail. The Mach disk and its trail could be seen on Fig. 2. The tangential discontinuity is observed behind the triple point. Its instability leads to formation of vortices and the zone of instant reverse flow (Fig. 3). However, the average velocity remains positive. The low-velocity zone is formed in the simulation behind the Mach disk. It could be seen on Fig. 4a where show the distribution of average longitudinal velocity referred to the U_j (adiabatic velocity at nozzle exit). The similar zone observed in the simulation [5] using LES on unstructured meshes containing 22×10^6 tetrahedral cells. In the experiment [16] the average velocity behind the Mach disc higher than in calculations. This discrepancy is explained in [5] both by the underestimation of the turbulence behind the Mach disc in the simulation and bias of DPIV in strong deceleration and sharp gradients.

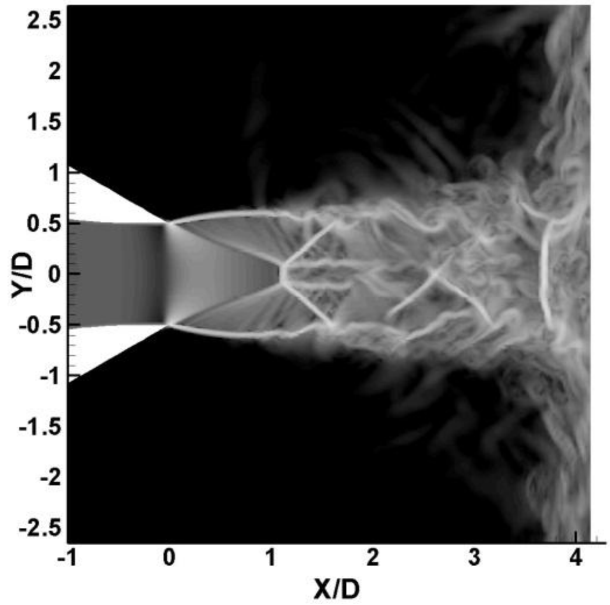

Fig. 2. Instantaneous distribution of $\log_{10}|grad\rho|$ in the X-Y plane, T_{in}=300K.

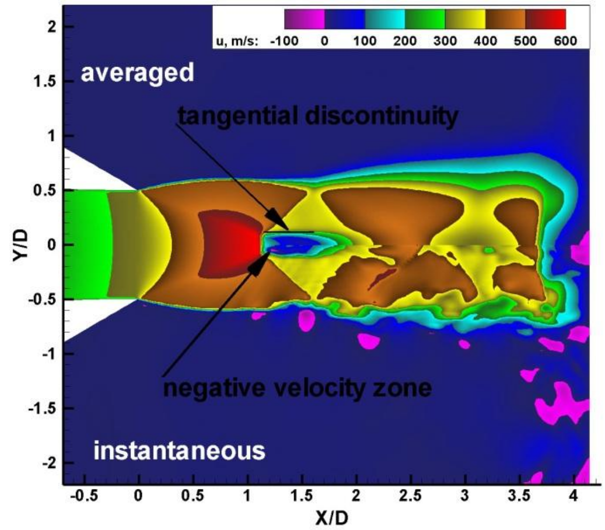

Fig. 3. Instantaneous and averaged distribution of longitudinal velocity in the X-Y plane, T_{in}=300K.

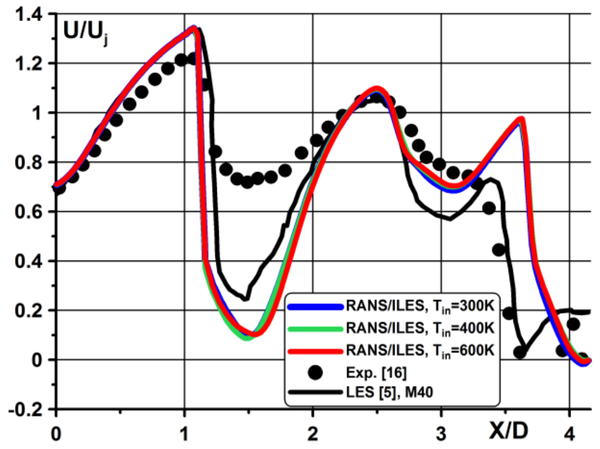

a) Averaged longitudinal velocity

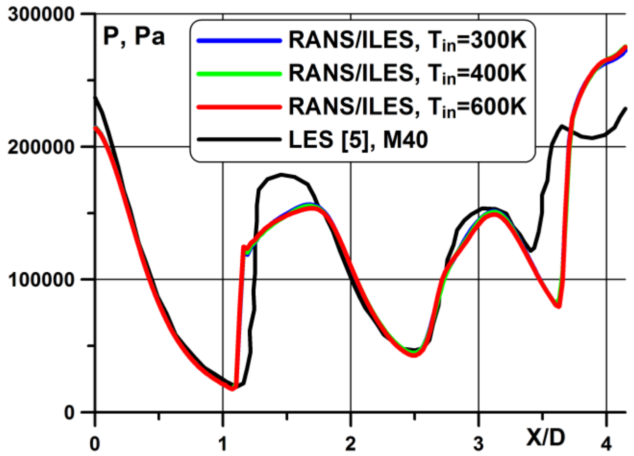

b) Averaged static pressure

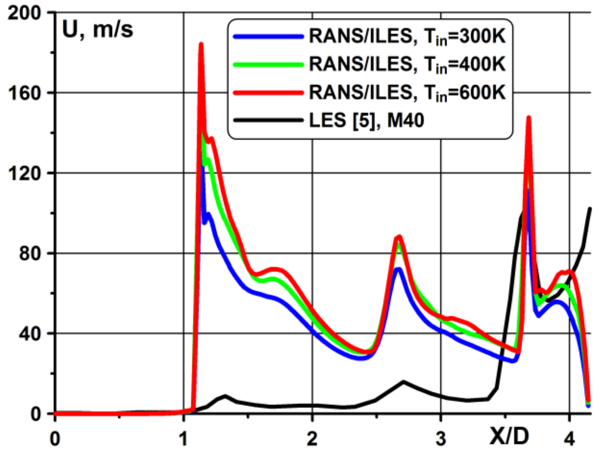

c) Longitudinal velocity fluctuation

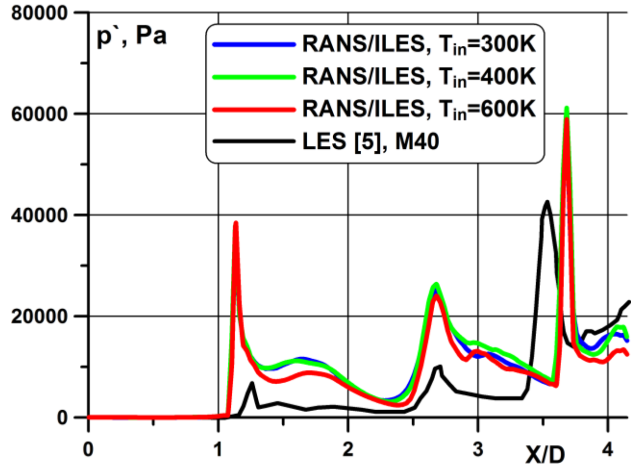

c) Static pressure fluctuation

Fig. 4. Distributions along the jet axis.

The averaged static pressure distribution at the jet axis (Fig. 4b) is in good agreement with the calculation of [5] with the exception of the area behind the Mach disc X/D = 1.5. In this simulation the magnitude of longitudinal velocity and static pressure fluctuations at the jet axis higher than in [5]. It could be seen on Fig. 4.This may be associated with the using in [5] additional viscosity at the shock waves to stabilize a central-difference scheme. Using slip conditions at the wall in [5] leads to a difference in the flow description near the plate (Fig. 4a, 4c and 5-6). In [5] the velocity at the wall and its fluctuations are not zero. Averaged static pressure in recirculation zone at the plate (Fig. 5) in current study higher than that in [5]. Also the maximum of static pressure fluctuation at the plate (Fig. 6) in this research is equal approximately 3000 Pa that in 1.75 times less than in [5]. Results of calculations by RANS/ILES and LES [5] outside of the recirculation zone are close to each other.

From Fig. 4-6 are seen that the changing T_{in} from 300 K to 600K influence on flow and turbulence parameters on the jet axis and the distribution of pressure and pressure fluctuation in the wall is negligible. This is due to that the

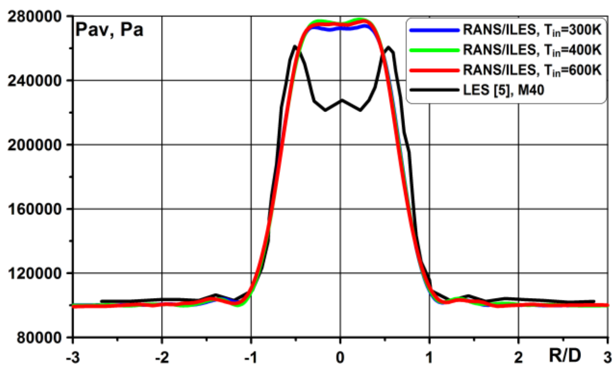

Fig. 5. Distributions of averaged static pressure along the plate.

changing of total temperature at the nozzle inlet with the constant NPR manifests itself as a changing the Reynolds number since the dynamic pressure is not changed (Table 1). The decreasing of Reynolds number from 1×10^6 to 0.64×10^6 is not affected on the supersonic jet flow. There is maximum of the distribution of turbulence kinetic energy (Fig 7) near the plate (X/D=4) at distance of 2D from jet axis. Its magnitude is decreased by 15 % with increasing temperature. Perhaps, this effect is due to the decreasing of the Reynolds number.

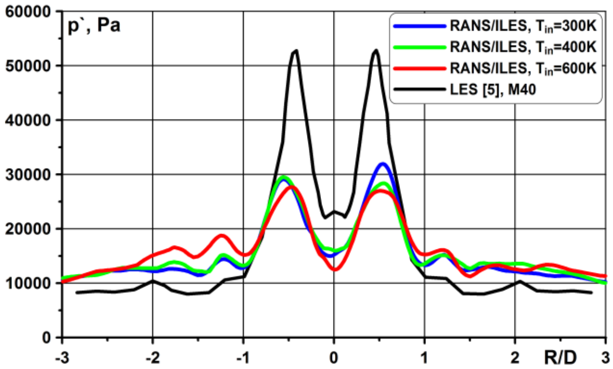

Fig. 6. Distributions of static pressure fluctuation along the plate.

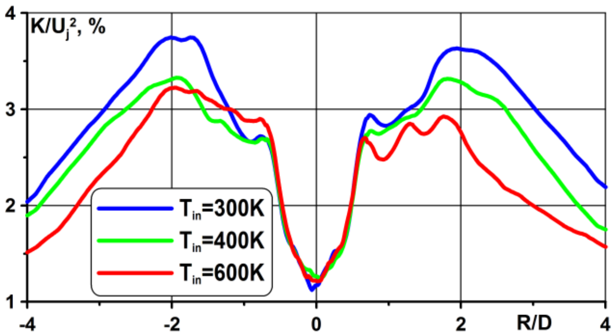

Fig. 7. Distribution of turbulence kinetic energy near the plate (X/D=4).

The jet temperature influence on the temperature and temperature fluctuations distribution on the wall are shown in Fig. 8 and 9. The distribution of averaged temperature and temperature fluctuation referred to the T_{in}. On the plate inside the recirculation zone, averaged temperature distribution independent on the T_{in} and the outside is aligned with the ambient temperature. The temperature fluctuations on the plate outside the recirculation zone behave nonmonotonically depending on the T_{in}. The temperature fluctuations maximum of the cold jet is located at R/D=3 and its magnitude is approximately by 1.8 times higher than that for the jet with T_{in} = 400K. For the jet with T_{in} = 600K the magnitude of fluctuation maximum is 4% which is slightly above than that for jet with T_{in}= 400K.

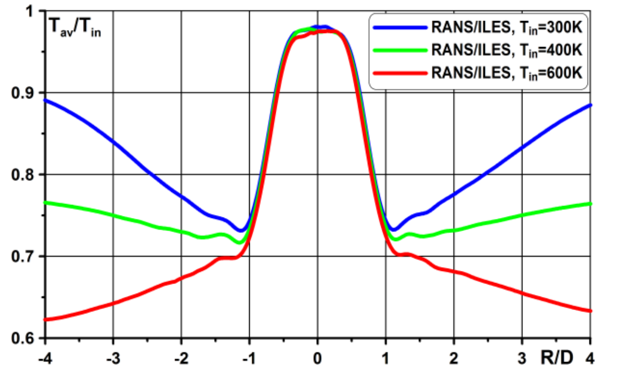

Fig. 8. Distributions of averaged static temperature along the plate.

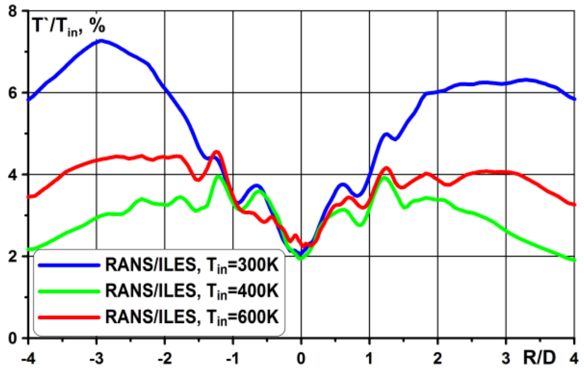

Fig. 9. Distributions of static temperature fluctuation along the plate.

Fig. 10 shows the static pressure fluctuation in sound pressure level (SPL) for the cold jet. The SPL is calculated by formula:

$$SPL = 20\log_{10}\left(\frac{p^{`}}{2\times10^{-5}}\right)$$

It can be seen that the maximum magnitude of fluctuation is located at the Mach disk, the contact line and on the wall at R/D = 0.5. The red line shown on Fig. 10 is used for the calculating distribution of overall sound pressure level (OASPL) in the near field of the jet (Fig 11). The noise level in the near field is increased by 1-3 dB with increasing temperature from 300K to 600K. The case with T_{in} = 400K have the noise level close to the jet with T_{in} = 600K.

The SPL spectrum of hot jets at the boundary of recirculation zone (X/D = 4.16, R/D = 0.5) (Fig. 12) is slightly lower than the cold jet. The maximum of cold jet spectrum is at St=0.2-0.4 (St – Strouhal number) and its level is more pronounced than that in cases with T_{in}=400K and 600K.

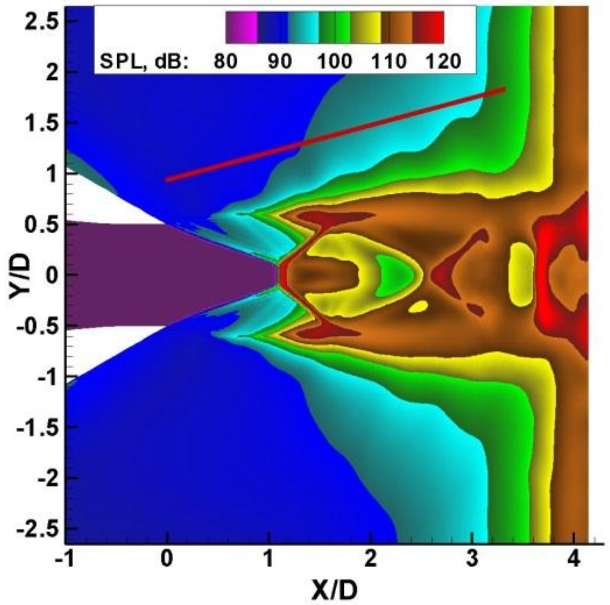

Fig. 10. Pressure fluctuation level in dB in the X-Y plane, T_{in}=300K.

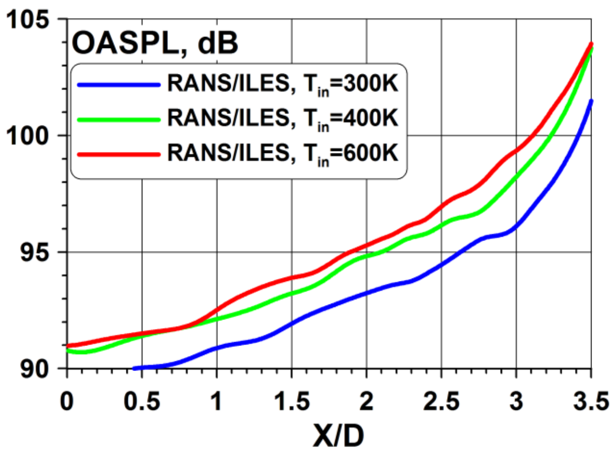

Fig. 11. Near-field overall sound pressure level distribution along line (0; 1D)-(3.5D; 2D) shown in Fig. 10.

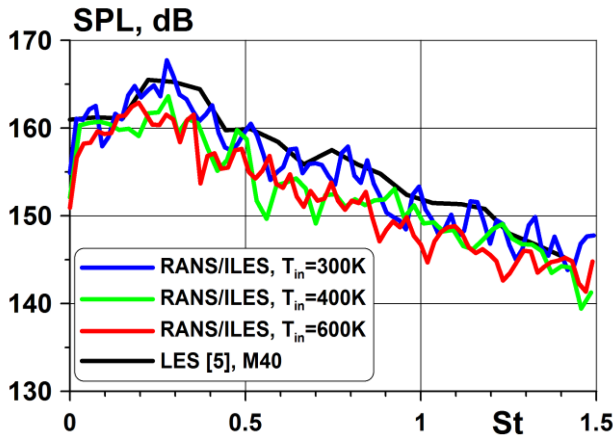

Fig. 12. Spectrum of static pressure fluctuation at the boundary of recirculation zone.

4 Conclusion

The influence of the total temperature at the nozzle inlet on the distribution of flow and turbulence parameters of supersonic impinging jets was considered using RANS/ILES- high-resolution method. The averaged flow parameters and characteristics of the turbulence on the jet axis and at the wall were considered. The good agreement with experiment [16] and calculations [5] was achieved. The T_{in} increase reduces the turbulence energy near the plate (R/D = 2) from 3.5% to 3%. Outside the recirculation zone the maximum magnitude of temperature fluctuations on the plate are changed approximately in 1.8 times depending on the T_{in} and shows nonmonotonous behavior. The overall level of noise in the near field for the hot jets is higher for approximately 1 – 3 dB, changing T_{in} from 400K to 600K did not gave a significant increase in noise level. There is maximum of impinging jets spectra at St=0.2 – 0.4 at the boundary of recirculation zone (X/D = 4.16, R/D = 0.5).

Acknowledgments

The work was supported by RFBR (grant number 12-08-00951-a). The author thanks Lyubimov D.A. for helpful discussions and comments.

References

1. M. Attalla, M. Salem, Effect of nozzle geometry on heat transfer characteristics from a single circular air jet. *Applied Thermal Engineering*, Vol. 51, pp. 723–733, 2013.
2. Jonas P. R. Gustavsson, Paul A. Ragaller, Rajan Kumar and Farrukh S. Alvi, Temperature Effect on Acoustics of Supersonic Impinging Jet. *AIAA 2010-3785*, 2010
3. Seiji Tsutsumi1, Ryoji Takaki, Yuta Nakanishi3, Koji Okamoto, Susumu Teramoto, Numerical Study on Acoustic Radiation from a Supersonic Jet Impinging to an Inclined Plate. *AIAA 2011-2922,* 2011
4. Nonomura, T., and Fujii, K., Computational Study of Effects of Near-wall Turbulent Structure on Aeroacoustics Fields of a Supersonic Jet Impinging on an Inclined Plate. *AIAA 2011-2917*, 2011.
5. Dauptain A., Cuenot B., Gicquel L. Y.M. Large Eddy Simulation of Stable Supersonic Jet Impinging on Flat Plate. *AIAA Journal*, Vol. 48. No. 10, pp. 2325–2338, 2010.
6. A. Dauptain, L. Y. M. Gicquel, S. Moreau, Large Eddy Simulation of Supersonic Impinging Jets. *AIAA Journal*, Vol. 50, No. 7, pp. 1560-1574, 2012.
7. Slawomir Kubacki, Erik Dick, Hybrid RANS/LES of flow and heat transfer in round impinging jets. *International Journal of Heat and Fluid Flow*, Vol. 32, pp. 631–651, 2012.
8. Lyubimov D.A. The application of hybrid RANS/ILES approach for the investigation of the effect of nozzle geometry and mode of efflux on the characteristics of turbulence of exhaust jets. *High Temperature*, Vol. 47, No 3, pp. 390–399.
9. Uzun A., Hussaini M.S. High-Fidelity Numerical Simulation of a Round Nozzle Jet Flow. *AIAA 2010–4016*, 2010.
10. Lyubimov D.A. Development and application of a high-resolution technique for jet flow computation using large eddy simulation. *High Temperature*, Vol. 50, No. 3, pp. 450-466.
11. Bendersky L. A., Lyubimov D.A. Using large-eddy simulation method for the research influence of total flow parameters at the nozzle inlet and off-design conditions on the flow and turbulence characteristics in a supersonic jet flowing out of biconical nozzles flow. *XVI International Conference on the Methods of Aerophysical Research*, Kazan, Russia, Vol. 1, pp. 47-48.
12. Suresh A., Huynh H. T. Accurate Monotonicity–Preserving Schemes with Runge-Kutta Time Stepping. *J. Comput. Phys*, Vol. 136, No. 1. p. 83, 1997.
13. Grinstein F.F., Margolin L.G., Rider W.J. *Implicit Large Eddy Simulation: Computing Turbulent Fluid Dynamics*. Cambridge University Press, 2007.
14. Spalart P.R., Allmaras S.R. A One-Equation Turbulence Model for Aerodynamic Flows. *La Recherche Aerospatiale*, No. 1. p. 5, 1994.
15. L.D. Landau, E.M. Lifshitz. *Fluid Mechanics*. Vol. 6 2nd edition, Butterworth-Heinemann,1987.
16. Henderson B., Bridges J., Wernet M. An experimental study of the oscillatory flow structure of tone-producing supersonic impinging jets. *J. Fluid Mech*., Vol. 542, pp. 115–137, 2005.

Copyright Statement